


Cite this: *RSC Adv.*, 2017, 7, 33914

# A novel experimental device for electrochemical measurements in supercritical fluids up to 700 °C/1000 bar and its application in the corrosion study of superalloy Inconel 740H

Sen Lin,<sup>a</sup> <sup>a</sup> Heping Li,<sup>\*a</sup> Liping Xu,<sup>a</sup> Yanqing Zhang<sup>b</sup> and Can Cui<sup>a</sup>

A three-electrode electrochemical study concerning electrically conductive materials submitted to supercritical fluids above 550 °C has not been reported in spite of its significance in many related fields. In this work, the design of a novel experimental device allowing three-electrode electrochemical measurements in high temperature and pressure fluids up to 700 °C/1000 bar is detailed described. In this device, pyrophyllite is used as a new electrode sealing material and the electrodes are sealed using a conical self-energizing sealing structure, which ensures the water tightness of the electrodes at pressures up to 1000 bar. The reference electrode in this device can either be an Ag/AgCl external pressure balanced reference electrode (EPBRE) or a platinum reference electrode. The potentiodynamic polarization plots and electrochemical impedance spectroscopy (EIS) of nickel-based superalloy Inconel 740H, a candidate material for Generation IV nuclear reactors, in deaerated water and chloride containing fluid (600–700 °C, 600–1000 bar) are presented using this device.

Received 10th April 2017  
Accepted 29th June 2017

DOI: 10.1039/c7ra04054g

rsc.li/rsc-advances

## Introduction

High temperature and pressure fluids exist widely in nature, industry, engineering, and scientific experiments, such as sea-floor hydrothermal activity,<sup>1,2</sup> water-rock interactions in the interior of the Earth,<sup>3</sup> supercritical water oxidation in wastewater treatment,<sup>4,5</sup> high temperature hydrometallurgy,<sup>6,7</sup> and the preparation of nano-materials in supercritical fluids.<sup>8</sup> Moreover, the temperatures and pressures of these fluids are fairly high in some cases, for example, large ultra-supercritical boilers utilized in power plants operate at 600 °C/300 bar.<sup>9</sup> The design concept of Generation IV nuclear reactors uses supercritical water as a coolant and the reactor outlet temperature can be as high as 620 °C. The temperatures and pressures of the hydrothermal fluids in the interior of the Earth can be even higher.<sup>10</sup> The electrochemical properties of high temperature and pressure fluids, as well as the electrochemical corrosion of the electrically conductive materials submitted to high temperature and pressure fluids, such as the high temperature alloys employed as structural materials, the metals and semi-conductors acting as the functional materials and the electric conductive minerals used as the raw materials in high temperature hydrometallurgy, have been crucial research

subjects in many related fields. Three-electrode electrochemical measurement is one of the only few *in situ* research methods that can be applied in the extreme environment of high temperature and pressure fluids, thus, it has attracted much attention from researchers. Unfortunately, reports in this field are relatively scarce for the challenges in building up experimental devices.<sup>11</sup>

The most critical challenge in building up experimental devices for three-electrode electrochemical measurement in high temperature and pressure fluids is how to guarantee the water tightness and the electric insulation between the autoclave and the electrodes. In the published reports, the electrodes were assembled in the autoclave by either cold zone sealing way or hot zone sealing way. In cold zone sealing way,<sup>12–15</sup> certain part of the autoclave was cooled down, naturally or cooling device assisted, then the electrodes were sealed in the cooled part with PTFE or other electrically insulating materials. So far, the highest temperature and pressure achieved by cold zone sealing way were 528 °C/345 bar.<sup>13</sup> However, the cold zone sealing way led to great temperature gradient in the autoclave, in that condition, the fluids in the autoclave could hardly reach equilibrium state, the electrodes response would also deviate from ideal condition, thus, the stability and reliability of the experimental results were doubtful. In hot zone sealing way, the temperature of the electrode sealing structure was the same as the rest part of the autoclave, such an isothermal sealing way avoided the problem of temperature gradient in the autoclave. However, the sealing materials used by previous researchers,

<sup>a</sup>Key Laboratory for High Temperature & High Pressure Study of the Earth's Interior, Institute of Geochemistry, Chinese Academy of Sciences, Lincheng West Road 99, Guiyang 550081, China. E-mail: liheping@vip.gyig.ac.cn

<sup>b</sup>National Laboratory for Clean Energy (DNL), Dalian Institute of Chemical Physics, Chinese Academy of Sciences, Zhongshan Road 457, Dalian 116000, China



inorganic glue<sup>16</sup> or polymer materials including Teflon,<sup>17,18</sup> PEEK,<sup>19</sup> limited the application of the three-electrode electrochemical measurement devices. The temperature resistance of polymer materials is usually unsatisfactory, for example, Teflon, the most commonly used sealing material, starts to decompose at temperatures above 320 °C. Thus, these devices could work only in subcritical conditions. Inorganic glue could be used at higher temperatures, X. Guan and D. D. Macdonald<sup>16</sup> used zirconia glue to seal the electrodes, their set-up could operate at 500 °C/300 bar, the highest record for hot zone sealing way in literature. But it should be mentioned that the component in inorganic glue might hydrolyze in certain electrolytes, which would pollute the electrolytes and lead to crevice corrosion of the electrodes.

Choosing a suitable reference electrode is another challenge for high temperature and pressure electrochemical measurement. EPBRE has been employed in the majority of high temperature electrochemical studies for its stability and the reproducibility electrode potential. The thermal liquid junction potential (TLJP) caused by the non-isothermal electrolyte bridge for EPBRE used in subcritical aqueous system has been extensively discussed by researchers.<sup>20–23</sup> However, the TLJP in supercritical fluids and the possible interfacial potential between the supercritical phase and the subcritical phase remain unresolved issues, normalizing of the measured potential in supercritical fluids is still a problem that now seems impossible to overcome. Another defect of EPBRE is the possibility of pollution of the experimental fluids by chloride ions,<sup>22</sup> which may skew the experimental results in the corrosion study of chloride sensitive materials. Platinum electrode is another frequently used reference electrode in high temperature and pressure electrochemical measurement.<sup>16,24</sup> It is stable and easy to use, however, shift of the electrode potential probably occurs when strong polarization of the working electrode changes the concentrations of hydrogen, oxygen, and hydrogen ions in the fluids, and it is difficult to normalize the measured potential in fluids with complex components. Both the EPBRE and platinum reference electrode exhibit disadvantages in their application in high temperature and pressure electrochemical measurement devices, which limits the application of these devices.

The operating temperatures and pressures of the reported experimental devices for three-electrode electrochemical measurement in high temperature and pressure fluids, whether in cold zone sealing way or in hot zone sealing way, could not satisfy the requirement of industry and scientific research today. The reference electrodes utilized in these devices also limited their application in high temperature and pressure electrochemical measurement. As a consequence, a new set-up that can operate at higher temperatures (above 550 °C) and pressures (above 345 bar) with more widely suitable reference electrode is urgently needed.

In the present work, a novel device for three-electrode electrochemical measurement in high temperature and pressure fluids is developed. In this device, the working and counter electrodes are sealed with a conical self-energizing sealing structure by pyrophyllite, which is highly stable and has high

electric insulating performance after heat treatment. The reference electrode in this device can be chosen from an Ag/AgCl EPBRE and a platinum reference electrode, according to the need of the experiment. The device allows to conduct three-electrode electrochemical measurement at temperatures up to 700 °C and pressures up to 1000 bar with high reliability. It can be applied to evaluate the corrosion resistance of metallic materials submitted to ultra-supercritical fluids, which is of significant importance in the material selection for advanced ultra-supercritical boilers<sup>25,26</sup> and Generation IV nuclear reactors,<sup>27,28</sup> the device can also be utilized to research the interaction between water and electrical conductive minerals in the interior of the Earth,<sup>29</sup> which helps to reveal the dissolution and transformation of the hydrothermal deposits. With the aid of this device, the corrosion behaviors of nickel-based superalloy Inconel 740H, a candidate material for Generation IV nuclear reactors, were investigated by potentiodynamic polarization and electrochemical impedance spectroscopy (EIS) studies.

## Instrumentation

### System setup

As mentioned in the Introduction, the design of an experimental device for three-electrode electrochemical measurement in high temperature and pressure fluids that can operate at 700 °C/1000 bar is described in this work. The device consists of a pressure control system, a temperature control system, and an electrochemical test station. The schematic of the device is shown in Fig. 1.

The pressure control system is composed of an electrolyte reservoir which is made from stainless steel 316L (Taiyuan Iron & Steel Co., Ltd.), a high pressure plunger pump (Chengdu Haipu Pump Co., Ltd., 3DSY750/120, accuracy  $\pm 6$  bar), an autoclave with three electrodes, a four-way connection (stainless steel 316L), a pressure sensor (Chengdutest Electronics Co., Ltd., CY201, accuracy  $\pm 1$  bar), and a safety valve (Jiangxi Hangbo Technology Development Co., Ltd., AQF-150). Experimental electrolyte is pumped into the autoclave from the electrolyte reservoir with the aid of the high pressure plunger pump, the pressure of the system is detected by the pressure sensor, and controlled by the amount of electrolyte pumped into the autoclave. The autoclave, high pressure pump, pressure sensor and safety valve are connected by the four-way connection.

The temperature control system comprises a tube-type heating furnace (Shanghai Y-feng Electrical Furnace Co., Ltd., SK2-5), a temperature regulator (Shanghai Y-feng Electrical Furnace Co., Ltd., AI-518P), and a k-type thermocouple. The

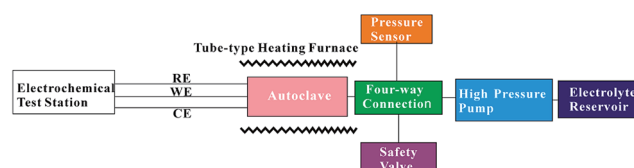


Fig. 1 The schematic of the experimental device for electrochemical measurement in ultra-supercritical fluids.



autoclave is placed in the isothermal region of the tube-type heating furnace, the measuring junction of the thermocouple is placed near the working electrode to make sure that the temperature measured by the thermocouple reflects the true temperature of the working electrode. Temperatures are controlled to  $\pm 0.5$  °C by the temperature regulator.

A Princeton 2263A electrochemical test station is employed to conduct electrochemical measurements.

### Autoclave

As shown in Fig. 2, the autoclave is made up of autoclave body and autoclave plug, a titanium sealing ring (Grade 1, Baotai Group Co., Ltd.) under the combined action of locknut, casing hold-down ring and tightening nut is used to ensure the water tightness between the autoclave body and the autoclave plug.

The chemical inertness of iron-based<sup>30,31</sup> and nickel-based<sup>32,33</sup> alloys in supercritical fluids is not satisfactory, especially in chloride-containing supercritical fluids, titanium alloy shows good chemical inertness in supercritical fluids,<sup>14</sup> but its mechanical performance is insufficiency. Thus, the autoclave body is designed to made out of nickel-based high temperature alloy Inconel 718 cylinder ( $d = 75$  mm,  $l = 200$  mm, Shanghai Baoyu Special Alloy Co., Ltd.) with a titanium alloy Ti-3Al-2.5V inside liner ( $d = 50$  mm,  $l = 188$  mm, Baotai Group Co., Ltd.), the thickness of the Inconel 718 shell and the Ti-3Al-2.5V inside liner are respectively 12.5 and 15 mm. Such a design not only guarantees the chemical inertness of the autoclave, but also provides good mechanical resistance,<sup>34,35</sup> the autoclave can operate at 700 °C and 1000 bar for long time run with large safety margins. The cylindrical cavity in the autoclave ( $d = 20$  mm,  $l = 90$  mm) has a volume of 28.26 mL. An internal thread hole ( $d = 14$  mm,  $l = 30$  mm) appears at the bottom of the autoclave body, through which the autoclave is connected to the four-way connection by a titanium capillary.

The autoclave plug (Fig. 3) is made out of Ti-3Al-2.5V bar ( $d = 24$  mm,  $l = 150$  mm, Baotai Group Co., Ltd.), the end which is placed into the autoclave body has three tapered bores inside, which are all 15 mm in depth and 12 degrees in angle, the diameter of their opening at the end surface are respectively 9.2, 9.2, and 8 mm. Each tapered bore is connected to an axial through-hole, which is 3 mm in diameter. The axial through-hole connected with the smaller tapered bore is internally threaded ( $d = 10$  mm,  $l = 20$  mm) at the other end, EPBRE is

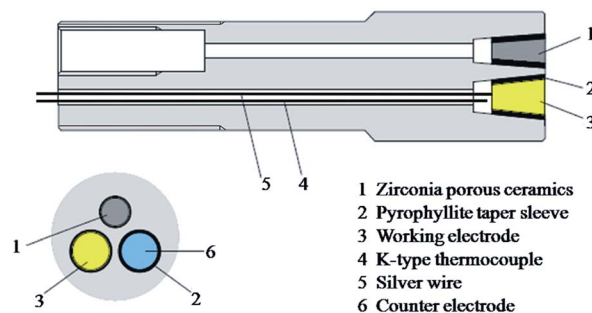


Fig. 3 The design of the autoclave plug and the assembling of the electrodes.

connected to the autoclave through this internal thread by a titanium capillary when EPBRE is employed as the reference electrode, a zirconia porous ceramics is placed in the smaller tapered bore as a salt bridge to separate the experimental fluid and the reference solution. While, in conditions that a platinum electrode is used as the reference electrode, the EPBRE is removed, and a platinum electrode is assembled in the smaller tapered bore instead of the zirconia porous ceramics. The working and counter electrodes are respectively assembled in the other two tapered bores.

### Working and counter electrodes

As mentioned above, shown in Fig. 3, the working and counter electrodes are assembled in the tapered bores at the autoclave plug. The working electrode is shaped into a cone frustum, which is 12 degrees in angle, and 10 mm in height. The diameters of the two end planes are respectively 7.2 and 5.1 mm, the larger end plane acts as the working surface, that is, the working electrode has an apparent working area of 0.41 cm<sup>2</sup>. The working electrode is sealed and electrically insulated from the autoclave plug with a 1 mm thick pyrophyllite taper sleeve (10 mm in height), which also has an angle of 12 degrees. The pyrophyllite taper sleeve together with working electrode cone frustum are inserted into the tapered bore at the autoclave plug with the aid of a hydraulic press machine. The working electrode cone frustum, the pyrophyllite taper sleeve, and the tapered bore at the autoclave plug make up a conical self-energizing sealing structure, such a design guarantees the water tightness of the electrode at pressures up to 1000 bar. A silver wire is held at the smaller end plane of the working electrode with high temperature resistant conductive adhesive, alumina ceramics tube is utilized to insulate the silver wire from the autoclave plug.

The counter electrode used in this work is a platinum electrode, its body is an alumina ceramics cone frustum with a platinum wire in its central axis, platinum powder is sintered on its both end planes, and the larger end plane is used as its working surface. The size and assembling manner of the counter electrode are the same as the working electrode.

The pyrophyllite taper sleeve shows excellent stability in high temperature and pressure fluids. We examined the pyrophyllite taper sleeve after respectively exposing to supercritical fluids

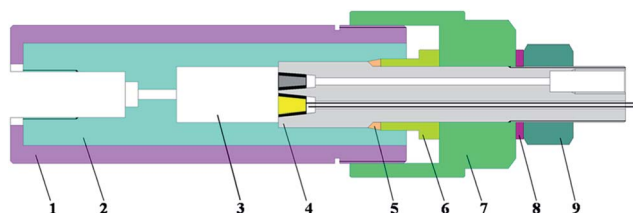


Fig. 2 The schematic of the autoclave with nickel based high temperature alloy shell (1), titanium alloy inside liner (2), cavity in the autoclave (3), titanium alloy autoclave plug (4), titanium sealing ring (5), casing hold-down ring (6), locknut (7), gasket (8), and tightening nut (9).



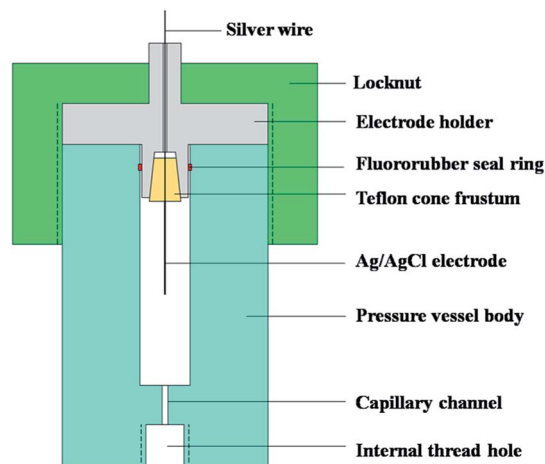


Fig. 4 The design of external pressure balanced Ag/AgCl reference electrode.

containing 0.01 M HCl and 0.5 M NaCl at 400 °C/1000 bar, 500 °C/1000 bar, 600 °C/1000 bar and 700 °C/1000 bar for 12 h, no sign of dissolution was observed.

### Reference electrode

The structure of the self-designed EPBRE is shown in Fig. 4. Ag/AgCl wire electrode is placed in the central axis of a Teflon cone frustum, which is then pressed into the tapered bore in the electrode holder (stainless steel 316L), the angle of the Teflon cone frustum and this tapered bore are both 12 degrees. The electrode holder is fixed with a locknut, a fluororubber seal ring is utilized to ensure the water tightness between the electrode holder and the pressure vessel body (stainless steel 316L). A titanium capillary connects EPBRE with the autoclave through the internal thread holes in the pressure vessel body of EPBRE and the autoclave plug. The cavity in EPBRE and the titanium capillary is filled with 0.1 M KCl. In subcritical conditions, the measured potential can be normalized with respect to saturated hydrogen electrode (SHE) using the equation proposed by Macdonald:<sup>20</sup>

$$E_{\text{SHE}}(T) = E_{\text{obs}} + 0.2866 - 0.001\Delta T + 1.745 \times 10^{-7}\Delta T^2 - 3.03 \times 10^{-9}\Delta T^3$$

When a platinum electrode is employed as the reference electrode in this device, the Ag/AgCl EPBRE is removed, and a platinum electrode is assembled in the smaller tapered bore instead of the zirconia porous ceramics. The structure and assembling manner of the platinum reference electrode are the same as the platinum counter electrode.

## Experimental

Electrochemical measurements were conducted using the described device. The working electrode was nickel-based superalloy Inconel 740H (Special Metals Corporation). Before it was assembled in the autoclave plug, the working surface of

the electrode was previously polished with 1000, 2500, and 5000 grit SiC paper in turn, then, washed by ethanol and ultrapure water. Proper amount of dried NaCl was put into the autoclave before the autoclave plug was assembled if needed. The air in the autoclave was driven out by high purity argon before heating. As the temperature achieved the set value, ultrapure water ( $18.2 \text{ M}\Omega \text{ cm}^{-2}$ , deaerated by high purity argon) was slowly introduced into the autoclave until the pressure reached the

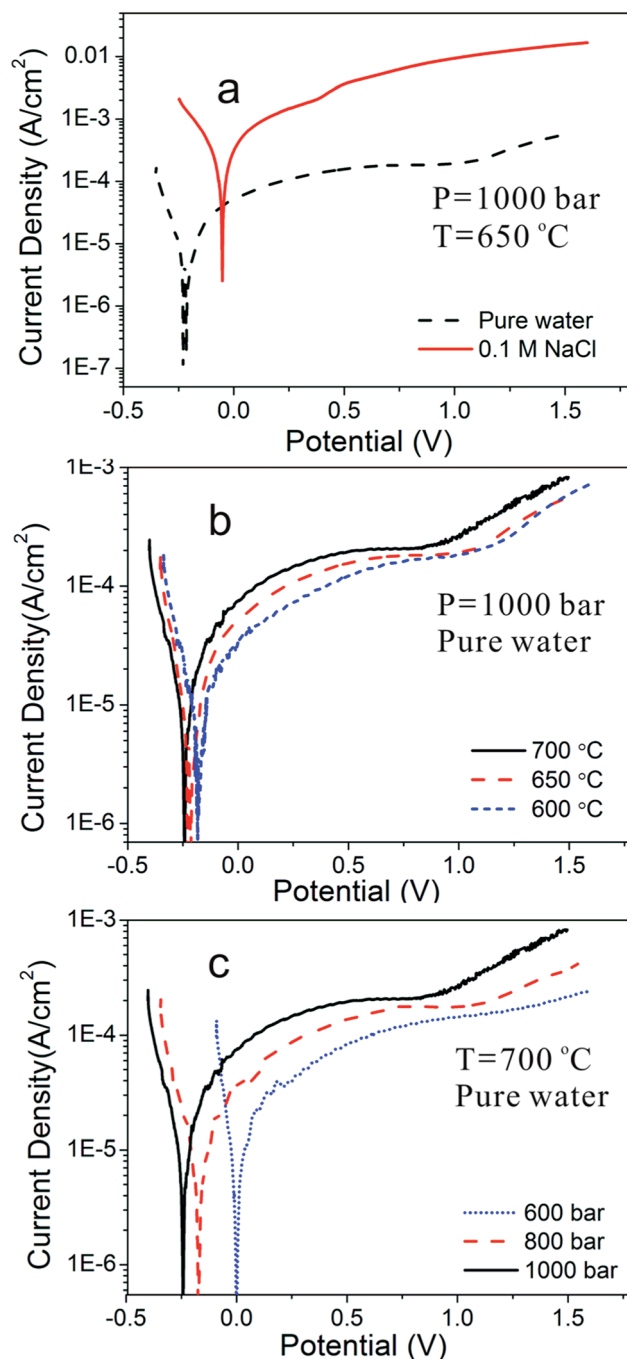


Fig. 5 Potentiodynamic polarization curves for alloy Inconel 740H in pure water and 0.1 M NaCl at 650 °C/1000 bar (a), in pure water with different temperatures at 1000 bar (b), and in pure water with different pressures at 700 °C (c), the scan rate is  $1 \text{ mV s}^{-1}$ .





desired value. Ag/AgCl EPBRE was employed as the reference electrode in this study, the potentials in this article were referenced to the EPBRE.

The electrochemical measurements were conducted using a Princeton 2263A electrochemical test station and Powersuit software. Potentiodynamic polarization plots were measured using a voltage scan rate of  $1 \text{ mV s}^{-1}$  from a point  $0.25 \text{ V}$  more negative than the open circuit potential. EIS measurements were conducted using an excitation voltage of  $10 \text{ mV}$  and an applied frequency from  $100 \text{ kHz}$  to  $10 \text{ mHz}$ .

## Results and discussion

The effects of chloride ions, temperature, and pressure on the corrosion behaviors of Inconel 740H were considered, potentiodynamic polarization and EIS studies were conducted in the temperature range of  $600$  to  $700^\circ\text{C}$  and pressure range of  $600$  to  $1000 \text{ bar}$ . To verify the reproducibility of the device, repeated experiments under the same experimental condition were conducted, the results overlap well with each other. Fig. 5a–c recorded the logarithm of the current as a function of the electrode potential under potentiodynamic polarization condition.

Fig. 5a shows the potentiodynamic polarization curves for Inconel 740H in pure water and  $0.1 \text{ M NaCl}$  solution at  $650^\circ\text{C}$ ,  $1000 \text{ bar}$ . In pure water, only one passivation current plateau is observed up to oxygen evolution and no dissolution–passivation

peak appears in the anodic branch. While, in  $0.1 \text{ M NaCl}$ , there is a significant increase in the current density when the potential is  $0.5 \text{ V}$  positive than the corrosion potential, which represents the starting of pitting corrosion. The current density in  $0.1 \text{ M NaCl}$  is over an order of magnitude higher than in pure water. Fig. 5b and c respectively reveal the potentiodynamic polarization curves in pure water at different temperatures and different pressures, and the potentiodynamic polarization curves are similar in shape. When the pressure is constant, in Fig. 5b, the current density values increases slightly with the increasing temperatures, and the oxygen evolution potential decreases with the increasing temperatures. While, when the temperature is constant, the current density values increases with the increasing pressures, and the oxygen evolution potential decreases with the increasing pressures (Fig. 5c).

Fig. 6a–c show the Nyquist plots for Inconel 740H after the electrode was hold at the test conditions for  $2 \text{ h}$ . A high frequency arc ( $100$ – $0.1 \text{ kHz}$ ) and a low frequency arc ( $100$ – $0.01 \text{ Hz}$ ) can be observed, which respectively represent the impedance of the passive film and the double layer at the electrode surface.<sup>36</sup> The equivalent circuit in Fig. 6d is employed to fit the EIS data, constant phase angle element (CPE) was used to replace the ideal capacitance  $C$  due to the surface roughness of the electrode.  $\text{CPE}_t/R_t$  represent the capacitance and resistance of the charge transfer double layer, they are in parallel with  $\text{CPE}_{pf}/R_{pf}$ , which represent the capacitance and resistance of the passive film at the electrode surface, and  $R_s$  is ohmic resistance

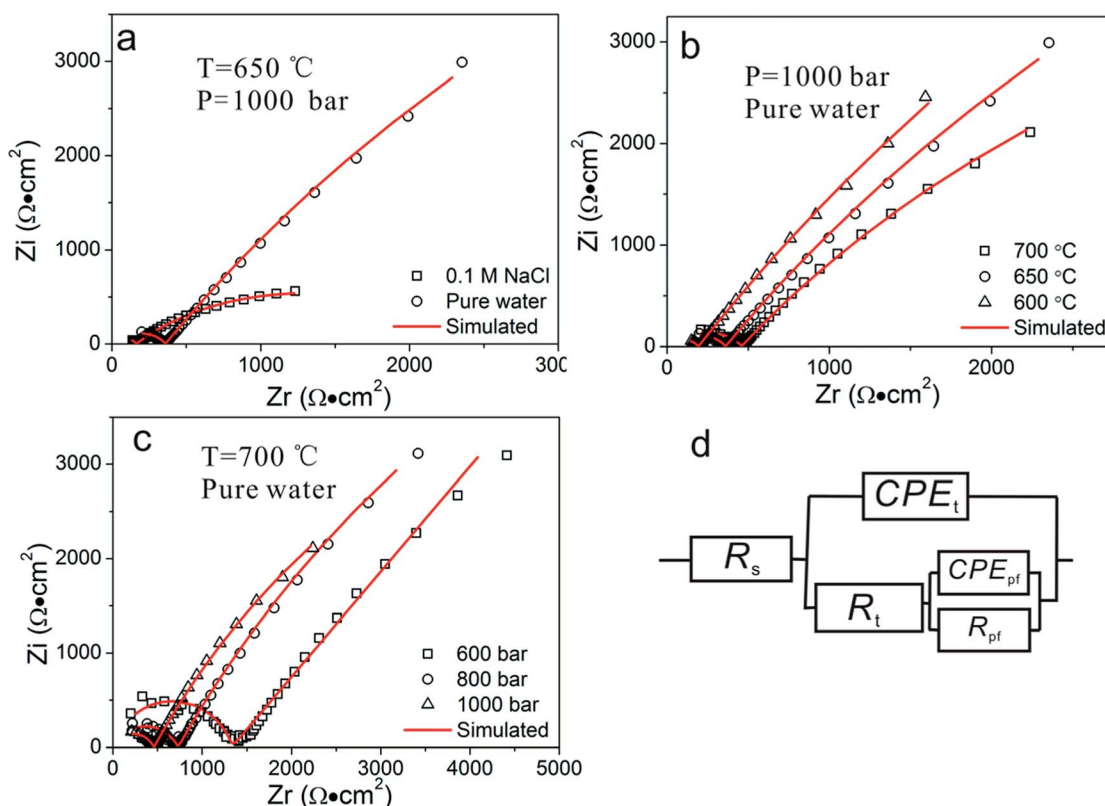


Fig. 6 Nyquist plots for alloy Inconel 740H in pure water and  $0.1 \text{ M NaCl}$  at  $650^\circ\text{C}/1000 \text{ bar}$  (a), in pure water with different temperatures at  $1000 \text{ bar}$  (b), in pure water with different pressures at  $700^\circ\text{C}$  (c), and the equivalent circuit (d).



of the circuit. The fitting results of  $R_t$  and  $R_{pf}$  are shown in Fig. 7. EIS measurements reveal that the presence of 0.1 M NaCl brings down both  $R_t$  (from 24.9 to 0.7) and  $R_{pf}$  (from 0.4 to 0.1  $\text{k}\Omega\text{cm}^2$ ) at a large scale. When the pressure is fixed at 1000 bar,  $R_t$  decreases from 32.1 to 14.6  $\text{k}\Omega\text{cm}^2$  and  $R_{pf}$  increases from 0.2 to 0.5  $\text{k}\Omega\text{cm}^2$  as the temperature increases from 600 to 700 °C (Fig. 6b). While, in the condition of a fixed temperature at 700 °C,  $R_t$  decreases from 105.6 to 14.6  $\text{k}\Omega\text{cm}^2$  and  $R_{pf}$  decreases from 1.1 to 0.5  $\text{k}\Omega\text{cm}^2$  as the pressure increases from 600 to 1000 bar (Fig. 6c).

The potentiodynamic polarization and EIS studies reveal that the addition of 0.1 M NaCl greatly promotes the corrosion of Inconel 740H. Firstly, the addition of NaCl improves the conductivity of the test fluid, benefitting the charge transfer step of the electrochemical reaction. Secondly, pitting corrosion tends to occur in the presence of chloride ions, which is confirmed by the morphology observation of the electrode surface after the test (Fig. 8). In pure water, the increase in pressure at a constant temperature results in the increase in dielectric constant, ionization constant and electrical conductivity, these changes are associated with greater ability for water to transport electrons and dissolve corrosion products, thus, increasing pressures at 650 °C promotes the corrosion of the

alloy, which is confirmed by both potentiodynamic polarization and EIS studies. The increase in temperature usually means a faster reaction speed, however, when the pressure is constant, increasing temperature also means lower density of supercritical water. At the pressure of 1000 bar, the densities of water at 600, 650 and 700 °C are respectively around 0.37, 0.32 and 0.28  $\text{g cm}^{-3}$ . The decrease in density results in the decrease in dielectric constant, ionization constant and electrical conductivity, which suppresses the corrosion of the alloy, and weakens the acceleration of corrosion speed by increasing temperature to some extent. Finally, the anodic current density in potentiodynamic polarization studies only increases slightly when temperature is increased from 600 to 700 °C.

## Conclusions

We present a novel experimental device allowing *in situ* electrochemical measurement in ultra-supercritical fluids in this work. The device contains a nickel based high temperature alloy Inconel 718 autoclave with titanium alloy Ti-3Al-2.5V inside liner, the electrodes are assembled in the hot zone at the autoclave plug, sealed by pyrophyllite taper sleeve with a conical self-energizing sealing structure. The reference electrode in this device can either be an Ag/AgCl EPBRE or a platinum reference electrode, which is according to the need of the experiment. The design of the device allows to perform three-electrode electrochemical measurement in high temperature and pressure fluids up to 700 °C/1000 bar for long time run, which fills in the blank of *in situ* electrochemical measurement in hydrothermal fluids above 550 °C. Potentiodynamic polarization and EIS studies for nickel-based superalloy Inconel 740H in the temperature range of 600 to 700 °C and the pressure range of 600 to 1000 bar showed that the presence of 0.1 M NaCl greatly promoted the corrosion of the alloy and led to pitting, while, the increased temperature and pressure both resulted in slightly increase in corrosion rate.

## Acknowledgements

This work was financially supported by the National Key Research and Development Plan (2016YFC0600100), 135 Program of the Institute of Geochemistry, CAS, and Large-scale Scientific Apparatus Development Program (YZ200720), CAS.

## Notes and references

- 1 R. A. Rona and S. D. Scott, *Econ. Geol. Bull. Soc. Econ. Geol.*, 1993, **88**, 1935–1976.
- 2 F. C. Tontini, T. J. Crone, C. E. J. de Ronde, D. J. Fornari, J. C. Kinsey, E. Mittelstaedt and M. Tivey, *Geophys. Res. Lett.*, 2016, **43**, 6205–6211.
- 3 A. G. Reyes and W. J. Trompetter, *Chem. Geol.*, 2012, **314**, 96–112.
- 4 M. D. Bermejo and M. J. Cocero, *AIChE J.*, 2006, **52**, 3933–3951.
- 5 S. J. Zhang, Z. H. Zhang, R. Zhao, J. J. Gu, J. Liu, B. Ormeci and J. L. Zhang, *Chem. Eng. Commun.*, 2017, **2**, 265–282.

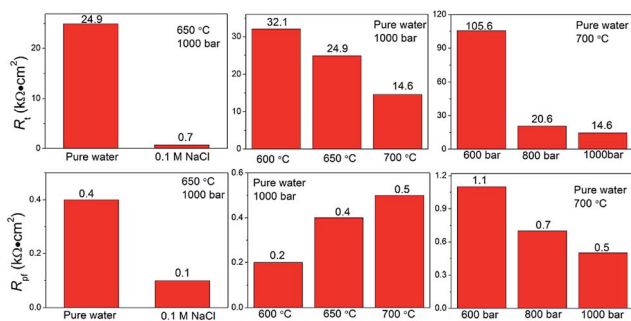


Fig. 7 Fitting results of  $R_t$  and  $R_{pf}$  for EIS measurements at different test conditions.

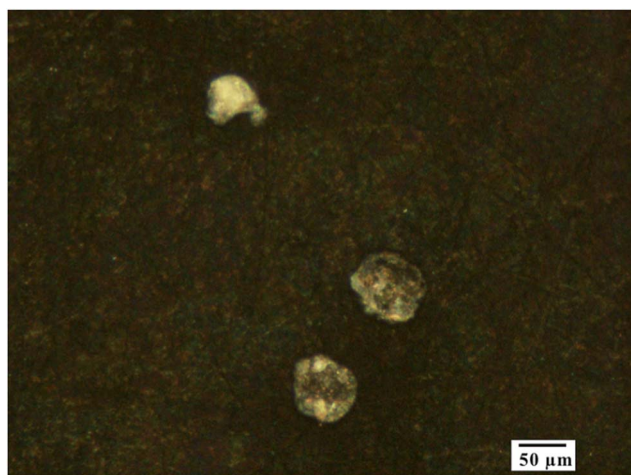


Fig. 8 Morphology image of the pitting corrosion for alloy Inconel 740H in 0.1 M NaCl fluids at 650 °C/1000 bar.



- 6 R. G. McDonald and D. M. Muir, *Hydrometallurgy*, 2007, **86**, 191–205.
- 7 C. M. Fleuriaux, C. G. Anderson and S. Shuey, *Miner. Eng.*, 2016, **98**, 161–168.
- 8 M. Golmohammadi, J. Towfighi, M. Hosseinpour and S. J. Ahmadi, *J. Supercrit. Fluids*, 2016, **107**, 699–706.
- 9 S. Espatolero, L. M. Romeo and C. Cortes, *Appl. Therm. Eng.*, 2014, **73**, 449–460.
- 10 R. R. Loucks and J. A. Mavrogenes, *Science*, 1999, **284**, 2159–2163.
- 11 G. G. Wildgoose, D. Giovanelli, N. S. Lawrence and R. G. Compton, *Electroanalysis*, 2004, **16**, 421–433.
- 12 H. Sun, X. Q. Wu and E. H. Han, *Corros. Sci.*, 2009, **51**, 2565–2572.
- 13 D. D. Macdonald and L. B. Kriksunov, *Electrochim. Acta*, 2001, **47**, 775–790.
- 14 P. Botella, F. Cansell, T. Jaszay, J. P. Frayret and M. H. Delville, *J. Supercrit. Fluids*, 2003, **26**, 157–167.
- 15 A. Couet, A. T. Motta, A. Ambard and D. Livigni, *Corros. Sci.*, 2017, **119**, 1–13.
- 16 X. Guan and D. D. Macdonald, *Corrosion*, 2009, **65**, 376–387.
- 17 D. D. Macdonald, J. Mankowski, M. Karaminezhad-Ranjbar and Y. H. Hu, *Corrosion*, 1988, **44**, 186–192.
- 18 Z. G. Duan, F. Arjmand, L. F. Zhang, F. J. Meng and H. Abe, *J. Solid State Electrochem.*, 2015, **19**, 2265–2273.
- 19 G. K. H. Wiberg, M. J. Fleige and M. Arenz, *Rev. Sci. Instrum.*, 2014, **85**, 085105.
- 20 D. D. Macdonald, A. C. Scott and P. Wentrczek, *J. Electrochem. Soc.*, 1979, **126**, 908–911.
- 21 S. N. Lvov and D. D. Macdonald, *J. Electroanal. Chem.*, 1996, **403**, 25–30.
- 22 S. H. Oh, C. B. Bahn and I. S. Hwang, *J. Electrochem. Soc.*, 2003, **150**, 321–328.
- 23 W. F. Bogaerts, *Electrochim. Acta*, 2016, **212**, 102–112.
- 24 K. K. Kasem and S. Jones, *Met. Rev.*, 2008, **52**, 100–106.
- 25 F. Sun, Y. F. Gu, J. B. Yan, Z. H. Zhong and M. Yuyama, *J. Alloys Compd.*, 2016, **657**, 565–569.
- 26 G. R. Holcomb, *Oxid. Met.*, 2014, **82**, 271–295.
- 27 D. Guzonas and R. Novotny, *Prog. Nucl. Energy*, 2014, **77**, 361–372.
- 28 D. J. Kim, G. G. Lee, D. J. Kim and S. J. Jeong, *J. Mater. Sci. Technol.*, 2013, **29**, 1184–1190.
- 29 M. Yamamoto, R. Nakamura, T. Kasaya, H. Kumagai, K. Suzuki and K. Takai, *Angew. Chem., Int. Ed.*, 2017, **56**, 5725–5728.
- 30 C. Fill and H. Tiltscher, *Mater. Corros.*, 1997, **48**, 146–150.
- 31 X. Gao, X. Q. Wu, Z. E. Zhang, H. Guan, E. H. Han, X. Gao, X. Q. Wu, Z. E. Zhang and H. Guan, *J. Supercrit. Fluids*, 2007, **42**, 147–163.
- 32 S. S. Hwang, H. P. Kim and J. S. Kim, *Corrosion*, 2003, **59**, 821–827.
- 33 R. Fujisawa, K. Nishimura, T. Nishida, M. Sakaiharu, Y. Kurata and Y. Watanabe, *Corrosion*, 2006, **62**, 270–274.
- 34 B. Veriansyah, J. D. Kim and J. C. Lee, *J. Ind. Eng. Chem.*, 2009, **15**, 153–156.
- 35 K. Sue, T. Ono, Y. Hakuta, H. Takashima, D. Nishio-Hamane, T. Sato, M. Ohara, M. Aoki, Y. Takebayashi, S. Yoda, T. Hiaki and T. Furuya, *Chem. Eng. J.*, 2014, **239**, 360–363.
- 36 J. M. L. Canut, S. Maximovitch and F. Dalard, *J. Nucl. Mater.*, 2004, **334**, 13–27.

